

Chapter 8

Pore Water Geochemistry and Quantification of Methane Cycling



Yu Hu

Abstract Owing to numerous scientific cruises in the past two decades, pore water data from more than 250 sites within gas hydrate and cold seep areas of the South China Sea have been reported. These investigated sites are mainly distributed in the Dongsha–Taixinan, Shenhu, and Qiongdongnan areas of the northern South China Sea, together with a few sites from the Beikang Basin of the southern South China Sea. Pore water geochemical profiles at these sites have been used to indicate fluid sources that are linked to gas hydrates and methane seepage, to distinguish the anaerobic oxidation of methane (AOM) from organoclastic sulfate reduction, to reveal fluid flow patterns, and to quantify the rates of AOM. As the pore water data accumulate over a broad area of the SCS, recent attempts have been made to quantify regional sulfate and methane cycling in the subseafloor of the northern South China Sea. This quantitative assessment on a regional scale highlights the importance of deep-sourced methane in governing subseafloor carbon and sulfur cycling along continental margins.

8.1 Introduction

Early diagenesis occurs once sediment particles are buried below the seafloor. Early diagenesis is mainly driven by the degradation of organic matter and oxidation of hydrocarbons. Discrimination between the primary signals from the water column and the products of early diagenetic reactions is critical when using marine sediments for paleoenvironmental reconstructions. The solid-phase and pore water analysis of marine sediments are two fundamental approaches for investigating early diagenesis (Schulz 2006). Solid-phase analysis has advantages in sample collection and storage and analytical procedures are generally easier to perform, thus producing more reliable results. However, this approach in most cases cannot distinguish whether diagenetic reactions are on-going or occurred in the past and provides no information about the rates and kinetics of the diagenetic reactions (Schulz 2006). This large gap

Y. Hu (✉)

College of Marine Sciences, Shanghai Ocean University, Shanghai 201306, China

e-mail: huyu@shou.edu.cn

© The Author(s) 2023

D. Chen and D. Feng (eds.), *South China Sea Seeps*,

https://doi.org/10.1007/978-981-99-1494-4_8

can be filled by pore water analysis, which provides a more immediate biogeochemical archive during early diagenesis. For instance, pore water analysis can be used to quantify the rates of methane-consuming and -producing reactions during early diagenesis. The methane-consuming reaction in marine sediments mainly refers to the anaerobic oxidation of methane (AOM) coupled with sulfate reduction, which is mediated by anaerobic methanotrophic archaea and associated sulfate-reducing bacteria (e.g., Boetius et al. 2000). AOM consumes more than 90% of ascending methane in marine sediments, thereby serving as an efficient filter that prevents the release of methane, a powerful greenhouse gas, into the ocean and atmosphere (Reeburgh 2007).

During the past two decades, extensive efforts on pore water analysis have been made to detect gas hydrates and methane seeps in the South China Sea (SCS). Consequently, a vast number of sediment cores with pore water data were collected from the SCS during numerous research cruises. Due to the significance of pore water sulfate data for tracing methane seepages and AOM, more than 250 sites with available pore water sulfate data on the continental slope and rise of the SCS have been investigated during the past two decades (Fig. 8.1; see references in Table 8.1). These investigated sites mainly focused on the areas where indications for cold seeps and gas hydrates were found, including the Dongsha–Taixinan, Shenhu, and Qiongdongnan areas in the northern SCS and the Beikang Basin in the southern SCS (Fig. 8.1; Table 8.1).

Early pore water geochemical work was mainly dedicated to tracing the sources of pore fluid linked to gas hydrates and methane seepages in the northern SCS (e.g., Jiang et al. 2005; Suess, 2005; Chuang et al. 2006, 2010; Deng et al. 2006; Lin et al. 2006; Yang et al. 2006, 2008a; Wu et al. 2007, 2010, 2011, 2013a, b; Huang et al. 2008). Later work with more analyzed pore water parameters allowed the identification of AOM from organoclastic sulfate reduction in the SCS (e.g., Luo et al. 2013; Hu et al. 2015, 2018, 2020; Liu et al. 2020; Gong et al. 2021). With the increase in the kinds of measured pore water parameters, numerical simulations, mainly reaction–transport models, have been used to quantify the rates of AOM in the SCS (e.g., Chuang et al. 2013; Ye et al. 2016; Feng et al. 2018b, 2019, 2020; Hu et al. 2018, 2019; Zhang et al. 2019; Liu et al. 2020; Zha et al. 2022). Reaction–transport models have also been applied to reveal fluid flow patterns by reproducing the complex shapes of pore water sulfate profiles (Chuang et al. 2013; Hu et al. 2019; Feng et al. 2021). Compared with the numerous investigated sites from the northern SCS, recent pore water studies have extended to the Beikang Basin of the southern SCS (Fig. 8.1; Feng et al. 2018b, 2021; Huang et al. 2022). With the accumulation of pore water data from a vast number of sites (Fig. 8.1), recent work has attempted to quantify regional sulfate and methane cycling in the seafloor of the northern SCS (Zhang et al. 2019; Hu et al. 2022). This chapter provides an overview of the progress of pore water geochemistry from the continental slope and rise of the SCS that is used for the indication of fluid sources, for the identification of AOM and fluid flow patterns, and for quantifying AOM rates and regional methane cycling.

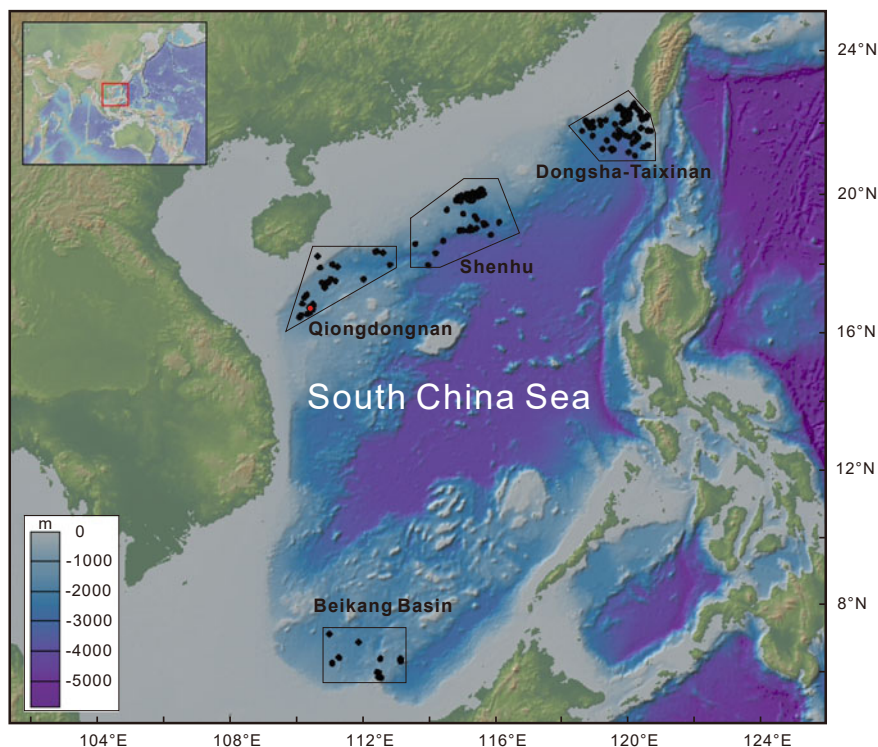


Fig. 8.1 Compilation of sites with available pore water data from the South China Sea. The red dot marks the position of the Haima cold seeps. Data sources were taken from the references listed in Table 8.1. The map was created using GeoMapApp software

Table 8.1 Published pore water data with positional information of gravity, piston, and push cores from the South China Sea. The sites of these cores are presented in Fig. 8.1

Areas	Site number	Core types	References
Dongsha–Taixinan	111	Gravity/piston	[1–14]
Shenhu	85	Gravity/piston/drilling	[15]
Qiongdongnan	46	Gravity/piston/drilling/push	[16–31]
Beikang Basin	11	Piston	[32–34]

Notes [1] Huang et al. 2008; [2] Wu et al. 2013a; [3] Suess, 2005; [4]Ye et al. 2016; [5] Hu et al. 2015; [6] Zhang et al. 2019; [7] Deng et al. 2006; [8] Zhang et al. 2014; [9] Hu et al. 2018; [10] Cao and Lei 2012; [11] Chen et al. 2017; [12] Chuang et al. 2013; [13] Hu et al. 2017; [14] Chuang et al. 2010; [15] Hu et al. 2022; [16] Feng et al. 2019; [17] Feng et al. 2020; [18] Wei et al. 2019; [19] Liu et al. 2020; [20] Yang et al. 2013; [21] Wu et al. 2010; [22] Feng et al. 2018a; [23] Wu et al. 2007; [24] Yang et al. 2006; [25] Jiang et al. 2005; [26] Luo et al. 2013; [27] Hu et al. 2019; [28] Hu et al. 2020; [29] Wang et al. 2018; [30] Hu et al. 2021; [31] Jin et al. 2022; [32] Feng et al. 2018b; [33] Feng et al. 2021; [34] Huang et al. 2022

8.2 Indication of Fluid Sources

Pore water geochemistry is a useful tool to indicate pore fluid sources in submarine cold seep environments. Because methane is the key component of the pore fluid, tracing methane sources and their linkage to gas hydrates thus becomes common issues of concern in areas influenced by methane seepages. Recent years have witnessed the discovery of gas hydrates by sampling and pore water geochemistry in the Dongsha, Shenhu, and Qiongdongnan areas (Yang et al. 2008b, 2015; Luo et al. 2014; Sha et al. 2015; Zhang et al. 2015; Liang et al. 2017; Hu et al. 2019; Wei et al. 2019; Ye et al. 2019). For instance, macroscopic gas hydrates have been found in shallow and deep marine sediments via piston and drill cores from the Qiongdongnan area (Fig. 8.2). Negative anomalies of pore water chloride concentrations relative to seawater value result from the dissociation of gas hydrates during sampling (Hu et al. 2019). In contrast, positive anomalies of pore water chloride concentrations reflect ongoing gas hydrate formation (Fig. 8.2; Wei et al. 2019). Once gas hydrates form in the sediment pore space from ambient water and dissolved methane, dissolved ions, such as pore water chloride, would be excluded as water molecules are incorporated into gas hydrates. This process increases the concentrations of pore water chloride, which in turn indicates the in situ formation of gas hydrates in the sediment pore space.

In shallow marine sediments, methane and other short-chain hydrocarbons mainly exist in the dissolved form in pore waters. These dissolved hydrocarbons can be collected using headspace vials for measuring their compositions. The carbon stable isotope ($\delta^{13}\text{C}$) values of methane are quite low, varying from -93‰ to -35‰ in marine sediments from the SCS (Fig. 8.3). The molecular ratios between methane and other short-chain hydrocarbons ($\text{C}_1/(\text{C}_1 + \text{C}_2)$) span four orders of magnitude (Fig. 8.3). The diagram of $\text{C}_1/(\text{C}_1 + \text{C}_2)$ ratios versus $\delta^{13}\text{C}$ values of methane is commonly used to distinguish biogenic methane that is bacterially generated in the methanogenic zone from thermogenic methane ascending from greater depths (Fig. 8.3). Methane in marine sediments of the southern SCS mainly originates from biogenic gas, while methane sources of the northern SCS are complex, with contributions from both biogenic and thermogenic methane (Fig. 8.3; Zhang et al. 2021; Huang et al. 2022). The ascending methane in marine sediments is largely consumed at the sulfate–methane transition zone (SMTZ), producing peak concentrations and $\delta^{13}\text{C}$ values of dissolved inorganic carbon (DIC) by AOM (Fig. 8.4; Hu et al. 2019). Based on the linear regression of $\delta^{13}\text{C} \times \text{DIC}$ versus DIC in cores QDN-14A and R1 of the Haima cold seeps, the estimated $\delta^{13}\text{C}$ values of DIC added to the pore water are -65‰ and -62‰ , respectively (Fig. 8.5). These $\delta^{13}\text{C}$ values are consistent with the $\delta^{13}\text{C}$ values of methane at the Haima cold seeps (Figs. 8.3 and 8.5). This observation suggests that DIC at the SMTZ is almost completely derived from highly ^{13}C -depleted methane by AOM at the Haima cold seeps.

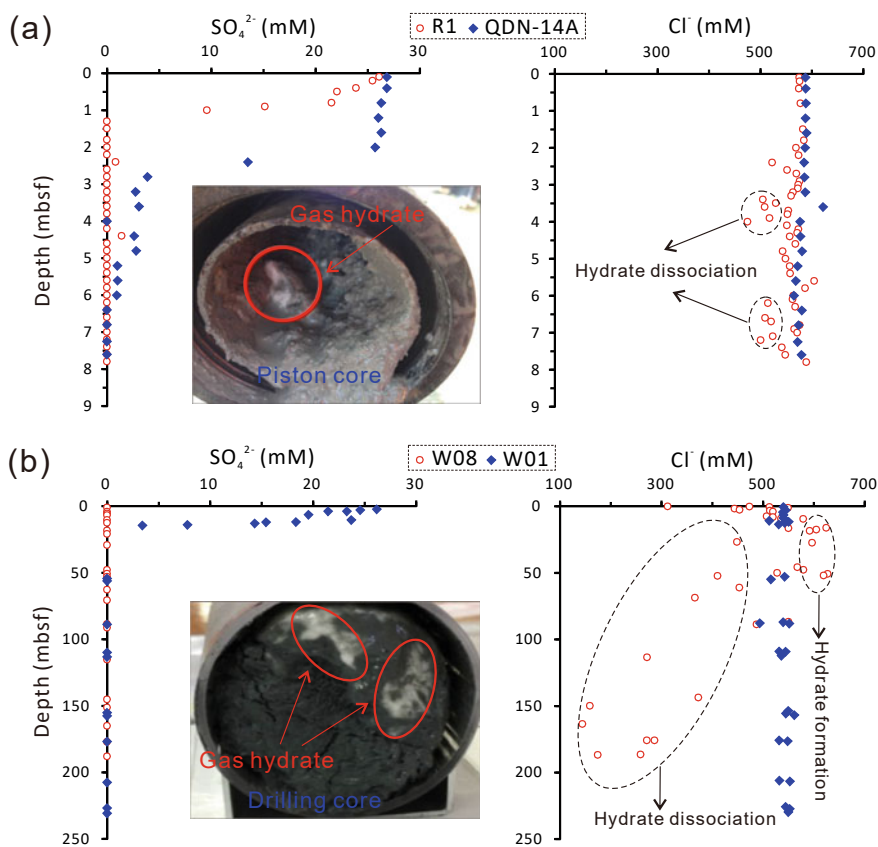


Fig. 8.2 Pore-water sulfate (SO_4^{2-}) and chloride (Cl^-) concentration profiles of (a) piston cores and (b) drill cores from the South China Sea. Piston cores R1 and QDN-14A were collected from the Haima cold seep, and drill cores W08 and W01 were recovered from the northeastern part of the Qiongdongnan Basin. The pore water data of the piston cores and drill cores were taken from Hu et al. (2019) and Wei et al. (2019), respectively. Photographs showing the presence of gas hydrates in the piston cores and drill cores were taken from Wei et al. (2019) and Liang et al. (2017), respectively. mbsf: meters below the seafloor

8.3 Identification of AOM

The extremely negative $\delta^{13}\text{C}$ values of DIC at the SMTZ could be used to identify the on-going AOM process (Fig. 8.4). However, this signature may be obscured by other DIC sources from organoclastic sulfate reduction and/or methanogenesis. Numerical models constrained by pore water sulfate, calcium, DIC, and nutrition concentrations and other parameters can be used to identify AOM and quantify the rates of AOM (e.g., Hu et al. 2018). Sulfur and oxygen isotopic patterns ($\delta^{34}\text{S}_{\text{SO}_4}$ versus $\delta^{18}\text{O}_{\text{SO}_4}$) of pore water sulfate have also been used to distinguish AOM from organoclastic sulfate reduction (e.g., Antler et al. 2015; Hu et al. 2020; Gong et al. 2021). However, the

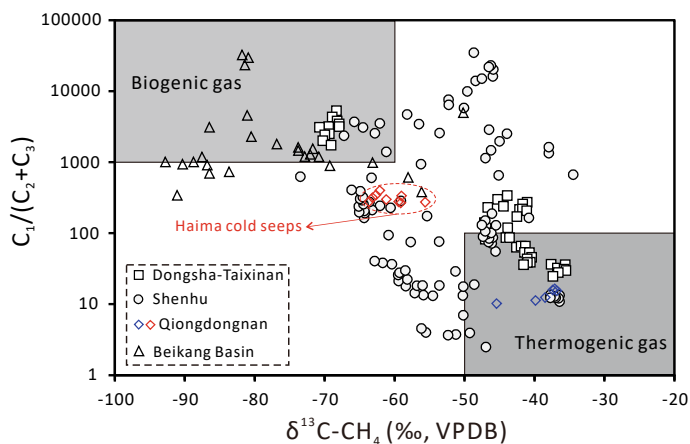


Fig. 8.3 Hydrocarbon compositions of sediment core samples compiled from numerous sites in the South China Sea. Molecular ratios between methane (CH_4) and other short-chain hydrocarbons ($C_1/(C_1 + C_2)$) and $\delta^{13}\text{C}$ data of CH_4 were taken from Zhang et al. (2021) and Huang et al. (2022)

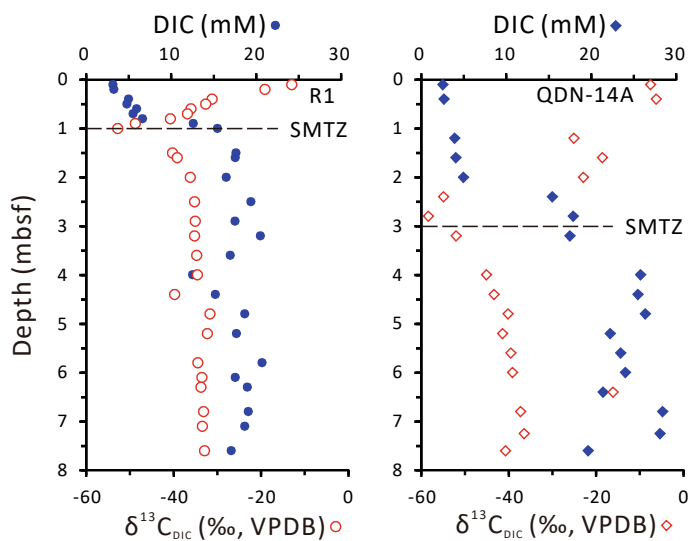


Fig. 8.4 Dissolved inorganic carbon (DIC) concentrations and carbon isotopic compositions of DIC ($\delta^{13}\text{C}_{\text{DIC}}$) in depth profiles of piston cores collected from the Haima cold seeps from the Qiongdongnan area (data from Hu et al. 2019). Sulfate–methane transition zone (SMTZ). mbsf: meters below the seafloor

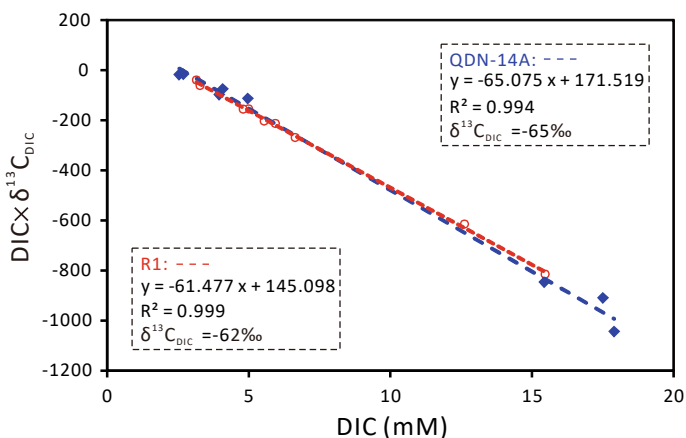


Fig. 8.5 Linear regression between dissolved inorganic carbon (DIC) and the $\delta^{13}\text{C} \times \text{DIC}$ of cores R1 and QDN-14A from the Haima cold seeps

numerical model approach requires numerous kinds of parameters, and the $\delta^{34}\text{S}_{\text{SO}_4}$ versus $\delta^{18}\text{O}_{\text{SO}_4}$ approach requires advanced analytical technology. The diagram of the produced DIC versus consumed sulfate ratios ($R_{\text{C:S}}$) after correcting for carbonate precipitation is widely used to identify AOM (Fig. 8.6; e.g., Luo et al. 2013; Hu et al. 2015, 2018, 2020 and references therein). This $R_{\text{C:S}}$ approach requires concentrations of only pore water sulfate, calcium, magnesium, and DIC.

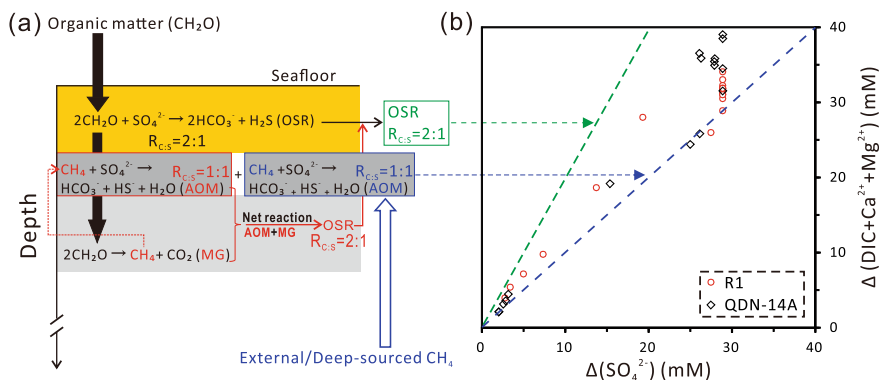


Fig. 8.6 Main biogeochemical processes in marine sediment and their control on the ratios ($R_{\text{C:S}}$) between produced dissolved inorganic carbon (DIC) corrected for carbonate precipitation and consumed sulfate (SO_4^{2-}). **a** Main biogeochemical processes responsible for $R_{\text{C:S}}$, including organo-oclastic sulfate reduction (OSR), anaerobic oxidation of methane coupled with sulfate reduction (AOM), and methanogenesis (MG). **b** Produced DIC corrected for carbonate precipitation ($\Delta(\text{DIC} + \text{Ca}^{2+} + \text{Mg}^{2+})$) versus consumed SO_4^{2-} (ΔSO_4^{2-}) relative to typical seawater values (2.1 mM for DIC, 10.3 mM for Ca^{2+} , 53.2 mM for Mg^{2+} , and 28.9 mM for SO_4^{2-}). Pore water data of R1 and QDN-14A were taken from Hu et al. (2019)

The $R_{C:S}$ approach is based on the reaction equations of organoclastic sulfate reduction and AOM that produce $R_{C:S}$ ratios equal to 2:1 and 1:1, respectively (Fig. 8.6a). However, this approach might be compromised by upward diffusive DIC from the methanogenic zone because methanogenesis below the SMTZ during preceding fermentation increases the DIC content of pore waters (Fig. 8.6a; e.g., Chatterjee et al. 2011; Kim et al. 2011; Hong et al. 2013; Hu et al. 2018). In addition to the addition of DIC from local methanogenesis to the SMTZ, methane produced by local methanogenesis is consumed by AOM when this methane diffuses into the SMTZ (Fig. 8.6a). The combined effect of these methane production and consumption processes around the SMTZ generates an $R_{C:S}$ of 2:1, which equals the $R_{C:S}$ of organoclastic sulfate reduction (Fig. 8.6a; Komada et al. 2016; Hu et al. 2018). Decoupled from local methanogenesis, methane without DIC at great depth (namely, external/deep-sourced methane) can migrate toward the SMTZ (c.f. Burdige and Komada 2013; Komada et al. 2016; Hu et al. 2018, 2022). This external/deep-sourced methane would be consumed by AOM when migrating into the SMTZ, thus generating an $R_{C:S}$ of 1:1 (Fig. 8.6a). Despite the potential interference from local methanogenesis, the $R_{C:S}$ approach is still useful to judiciously discriminate AOM from organoclastic sulfate reduction and/or methanogenesis (Fig. 8.6). If local methanogenesis occurs, the $R_{C:S}$ approach would result in an underestimation of AOM, thus representing a conservative approach to identify the presence of AOM and the deep-sourced methane (Fig. 8.6; Hu et al. 2018). Discrimination using the $R_{C:S}$ approach has been conducted in the areas of Dongsha–Taixinan (Hu et al. 2015, 2018), Shenhu (Hu et al. 2018, 2020), and Qiongdongnan (Luo et al. 2013; Liu et al. 2020; this study is shown in Fig. 8.6b). The results from these areas show much lower $R_{C:S}$ ratios of less than 2:1 or $R_{C:S}$ ratios approaching 1:1, revealing the occurrence of AOM (Luo et al. 2013; Hu et al. 2015, 2018, 2020). For instance, piston cores from the Haima cold seeps of the Qiongdongnan area exhibit $R_{C:S}$ ratios approaching 1:1, suggesting the dominance of AOM at the SMTZ (Fig. 8.6b). This inference is in accordance with the observation of extremely ^{13}C -depleted DIC at the SMTZ that almost completely results from AOM.

8.4 Implication for Fluid Flow Patterns

The changes in methane flux, physical mixing due to bioirrigation or bubble irrigation, and mass-wasting events create non-steady state depositional and/or environmental conditions (e.g., Fossing et al. 2000; Zabel and Schulz 2001; Hensen et al. 2003; Kasten et al. 2003; Hu et al. 2019 and references therein). This methane seepage variability and fluid flow patterns can be imprinted in pore water compositions in depth profiles (Hu et al. 2019). In particular, pore water sulfate profiles can exhibit changeable gradients ranging from kink to concave-up to s-types (e.g., Zabel and Schulz 2001; Hensen et al. 2003; Haeckel et al. 2007). Therefore, insights into the geochemical trends of pore water profiles can in turn reveal fluid flow patterns and possible sedimentary events (e.g., Hensen et al. 2003; Hu et al. 2019). Sulfate

and iodide concentrations remain nearly unchanged relative to seawater values in the upper 1–3 m of sediment cores at many sites from the Dongsha–Taixinan area of the SCS (Chuang et al. 2013). This irrigation-like feature could be attributed to meter-scale bioirrigation of macrofauna or seawater intrusion during methane ebullition (Fossing et al. 2000). However, this possibility is eliminated since bioirrigation usually occurs only on a decimeter scale in surface sediments (c.f. Haeckel et al. 2007; Hu et al. 2019). The irrigation-like feature is simulated by numerical modeling, assuming methane gas bubble irrigation with seawater, as proposed by Haeckel et al. (2007). The irrigation-like feature of pore water from the Dongsha–Taixinan areas is thus interpreted to reflect the irrigation of seawater by methane gas bubbles that rise through soft surface sediments (Chuang et al. 2013).

Similar irrigation-like features have also been observed in the upper 2 m of pore water profiles at the Haima cold seeps from the Qiongdongnan area (Fig. 8.7; Hu et al. 2019). The numerical model of methane bubble irrigation reproduced measured parameters in pore water profiles (Hu et al. 2019). The core near the seepage center (R1) with a higher methane flux is more susceptible to gas ebullition than cores that are relatively far away from the seepage center (QDN-14A and QDN-14B). It is paradoxical that the core near the seepage center has less indication of gas bubble irrigation (Fig. 8.7), making bubble irrigation unlikely to be the cause of the irrigation-like feature. Instead, the irrigation-like feature is attributed to enhanced methane fluxes from a combination of the lateral and upward migration of methane-rich fluids (Fig. 8.7). This situation is also reproduced by a non-steady-state numerical model (Fig. 8.7a). The presence of gas hydrates in core R1 can serve as a barrier for the upward movement of methane-rich fluids toward the seafloor and can laterally redirect the fluid flow (Fig. 8.7b). This lateral fluid flow is also promoted by the occurrence of coarser sediments in intervals directly below the SMTZ in cores QDN-14B and QDN-14A (Fig. 8.7b; Hu et al. 2019). In other words, the sealing of gas hydrate layers in core R1 redirected the pathway of upward-migrated methane-rich fluids from below the hydrate layers. The lateral migration of methane along with upward-migrated methane suddenly increased methane fluxes in nearby cores, resulting in the observed irrigation-like feature (Fig. 8.7b; Hu et al. 2019).

8.5 Quantifying AOM Rates and Regional Methane Cycling

The anaerobic oxidation of methane (AOM) consumes sulfate, with a stoichiometry of 1:1, thereby competing with organoclastic sulfate reduction above the SMTZ (Fig. 8.6a). Therefore, the values of AOM rates are usually lower than those of total sulfate reduction or sulfate diffusive flux. Methane concentration gradients below the SMTZ can be used to estimate AOM rates. Studies of only some sites from limited areas of the SCS have reported methane concentration data (e.g., Wu et al. 2011, 2013b; Chuang et al. 2013; Chen et al. 2017; Hu et al. 2020; Huang et al. 2022). On the other hand, the risk of underestimating AOM rates exists by using methane concentration gradients due to the rapid decrease in pressure and thereby possible

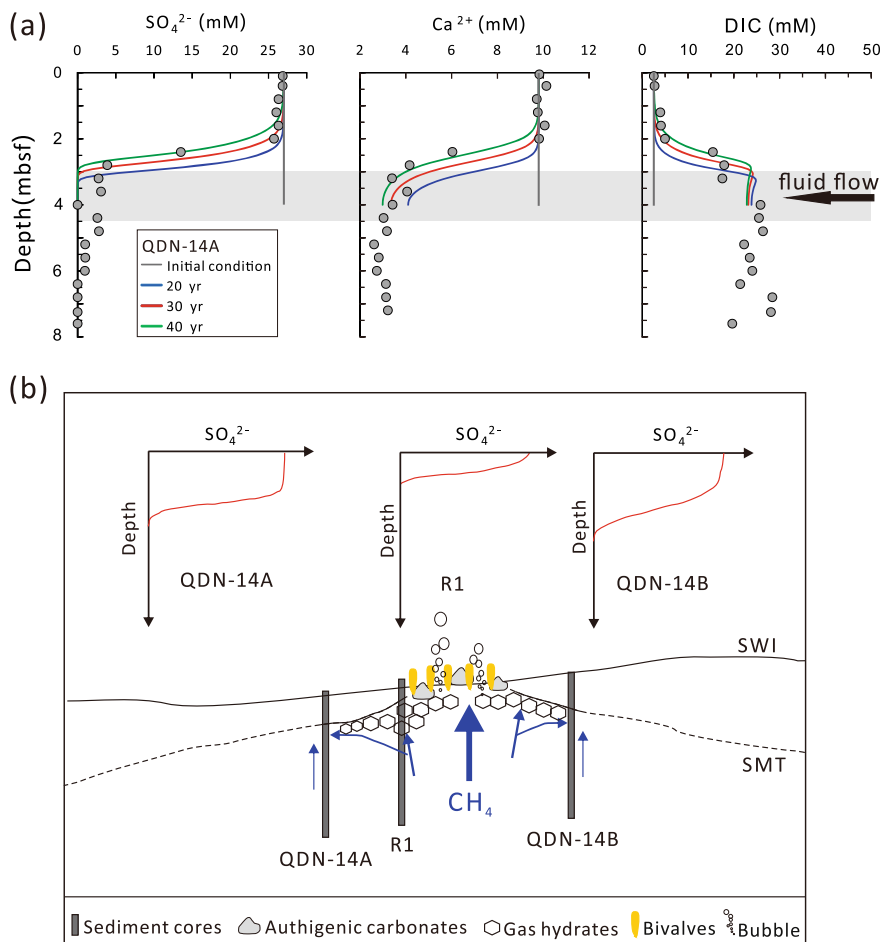


Fig. 8.7 Impact of flow fluid patterns on the shape of pore water sulfate (SO_4^{2-}) profiles (Modified from Hu et al. 2019). **a** Evolution of SO_4^{2-} , calcium (Ca^{2+}), and dissolved inorganic carbon (DIC) profiles over time from non-steady-state simulations of core QDN-14A that assume enhanced methane (CH_4) fluxes resulting from vertical and lateral fluid migration. **b** Schematic diagram showing flow fluid patterns as revealed by the shape of pore water SO_4^{2-} profiles. mbsf: meters below the seafloor. Reprinted from Marine and Petroleum Geology, 103, Hu et al. (2019) Pore fluid compositions and inferred fluid flow patterns at the Haima cold seeps of the South China Sea, 29–40, Copyright (2019), with permission from Elsevier

loss of methane during core recovery. Consequently, the attempt to use methane concentration gradients to constrain AOM rates is not common in the SCS (e.g., Chen et al. 2017; Hu et al. 2020). The rates of AOM can be more directly determined by a radiotracer approach using ^{14}C -labeled methane; however, this approach is rarely used in the SCS (Zhuang et al. 2019). In contrast, the reaction–transport model has been commonly used to quantify the AOM rates at sites in the Dongsha–Taixinan,

Shenhu, Qiongdongnan, and Beikang Basins by fitting numerous kinds of pore water parameters (e.g., Chuang et al. 2013; Ye et al. 2016; Feng et al. 2018b, 2019, 2020; Hu et al. 2018, 2019; Zhang et al. 2019; Liu et al. 2020; Zha et al. 2022). Of all the reported AOM rates, depth-integrated AOM rates at the Haima cold seeps are the highest (Hu et al. 2019; Liu et al. 2020). Due to shallow SMTZs at the Haima cold seeps from ~0.2 to 1 m below the seafloor (mbsf), the AOM rates exceed one thousand $\text{mmol m}^{-2} \text{a}^{-1}$ (Hu et al. 2019; Liu et al. 2020).

Despite more precision for quantifying AOM rates using reaction–transport models, very few sites from the SCS have been investigated (Zhang et al. 2019). 253 sites with available pore water data have been compiled from the SCS (Fig. 8.1; Table 8.1); however, most of these sites have only sulfate data, which limits the application of the reaction–transport model. These 253 sites all show a clear depth trend in sulfate concentration profiles, thereby allowing for the calculation of the SMTZ depth and reliable diffusive sulfate fluxes. Because sulfate fluxes generally represent the upper limit of AOM rates, the distribution of sulfate fluxes is helpful to constrain the regional AOM rates and methane cycling in the SCS. Sulfate profiles at 85 sites from the Shenhu area reveal that the depths of the SMTZ range from 6.6 to 88.5 mbsf (Hu et al. 2022). By using Fick’s first law, estimated sulfate fluxes vary from 2.4 to 30.7 $\text{mmol m}^{-2} \text{a}^{-1}$, with an average of 14.3 $\text{mmol m}^{-2} \text{a}^{-1}$ (Fig. 8.8a; Hu et al. 2022). Based on sulfate profiles of 111 sites from the Dongsha–Taixinan area (Fig. 8.1), the depths of the SMTZ range from ~0.4 to 43.0 mbsf, and estimated sulfate fluxes average 34.8 $\text{mmol m}^{-2} \text{a}^{-1}$, varying from 2.9 to 170.7 $\text{mmol m}^{-2} \text{a}^{-1}$ (Hu et al. 2023). From sulfate profiles at 46 sites in the Qiongdongnan area (Fig. 8.1), the depths of the SMTZ range from 0.2 to 111.2 mbsf, and estimated sulfate fluxes vary from 1.6 to 1203.4 $\text{mmol m}^{-2} \text{a}^{-1}$, with an average of 136.4 $\text{mmol m}^{-2} \text{a}^{-1}$ (Hu et al. 2023). The depths of the SMTZ at 11 sites from the Beikang Basin range from 3.3 to 8.8 mbsf (Fig. 8.1; Feng et al. 2018b, 2021; Huang et al. 2022). By spatial interpolation, the regional sulfate flux estimated from sulfate profiles in the Shenhu area is $0.54 \times 10^{-3} \text{Tmol a}^{-1}$ (Hu et al. 2022). In contrast, regional sulfate fluxes estimated from sulfate profiles at 111 sites from the Dongsha–Taixinan area and 46 sites from Qiongdongnan area are much higher, reaching 1.07×10^{-3} and $2.65 \times 10^{-3} \text{Tmol a}^{-1}$, respectively (Hu et al. 2023; Figs. 8.9, 8.10 and 8.11).

Deep-sourced methane can be identified by the $R_{C:S}$ approach, as shown in the diagram in Fig. 8.6. The amount of such deep-sourced methane on a regional scale has been recently quantified by the difference between the regional sulfate flux estimated from sedimentation rates and that from sulfate profiles (Hu et al. 2022). Sedimentation rates can be used to estimate sulfate fluxes based on the common good global correlation between diffusive sulfate fluxes and sedimentation rates, generating a global map for the distribution of sulfate diffusive flux (Egger et al. 2018). Sedimentation rates reflect the control of organic matter and sediment ages on the diffusive sulfate flux to the SMTZ, which is determined by the continuous decrease in the reactivity of organic matter with sediment depth (Egger et al. 2018 and references therein). Sulfate fluxes estimated from sedimentation rates thus represent sulfate consumption during organic matter degradation (Hu et al. 2022). This sulfate consumption includes (1) sulfate consumed by organoclastic sulfate reduction above the SMTZ

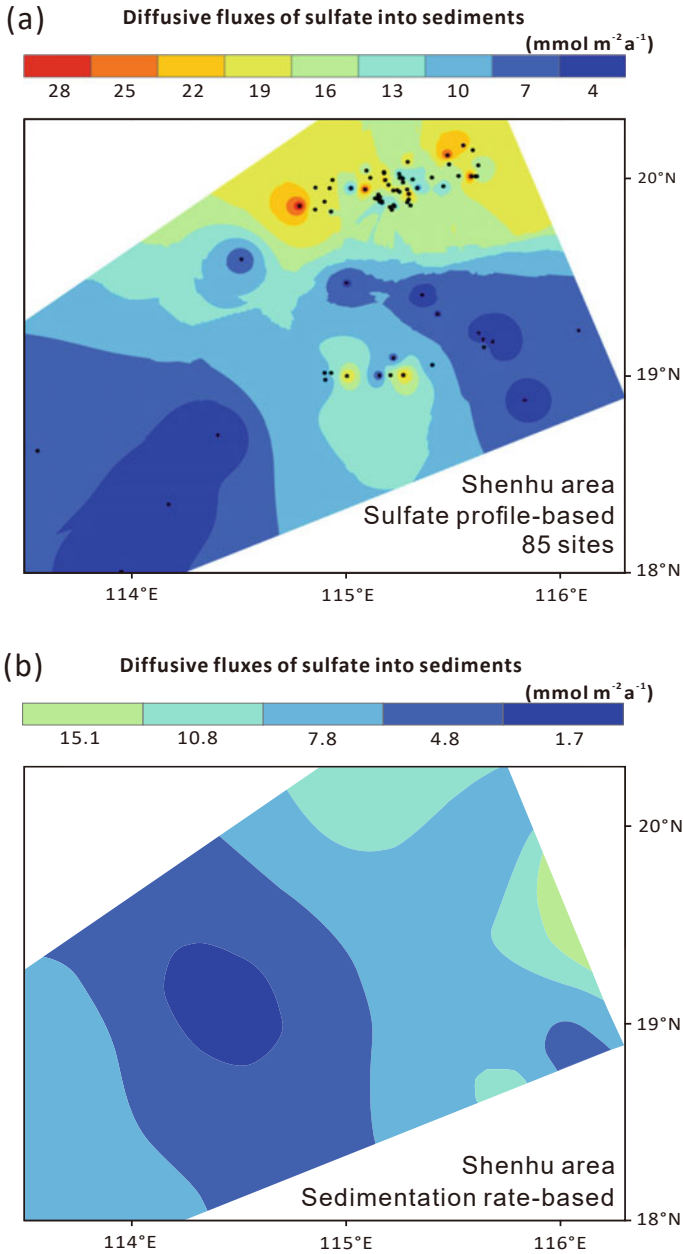


Fig. 8.8 Maps showing the distribution and magnitude of the regional sulfate flux of the Shenhu area based on measured sulfate profiles at 85 sites (a) and sedimentation rates (b), respectively (Modified from Hu et al. 2022). Reprinted from Science Bulletin, 67, Hu et al. (2022) Enhanced sulfate consumption fueled by deep-sourced methane in a hydrate-bearing area, 122–124, Copyright (2022), with permission from Elsevier

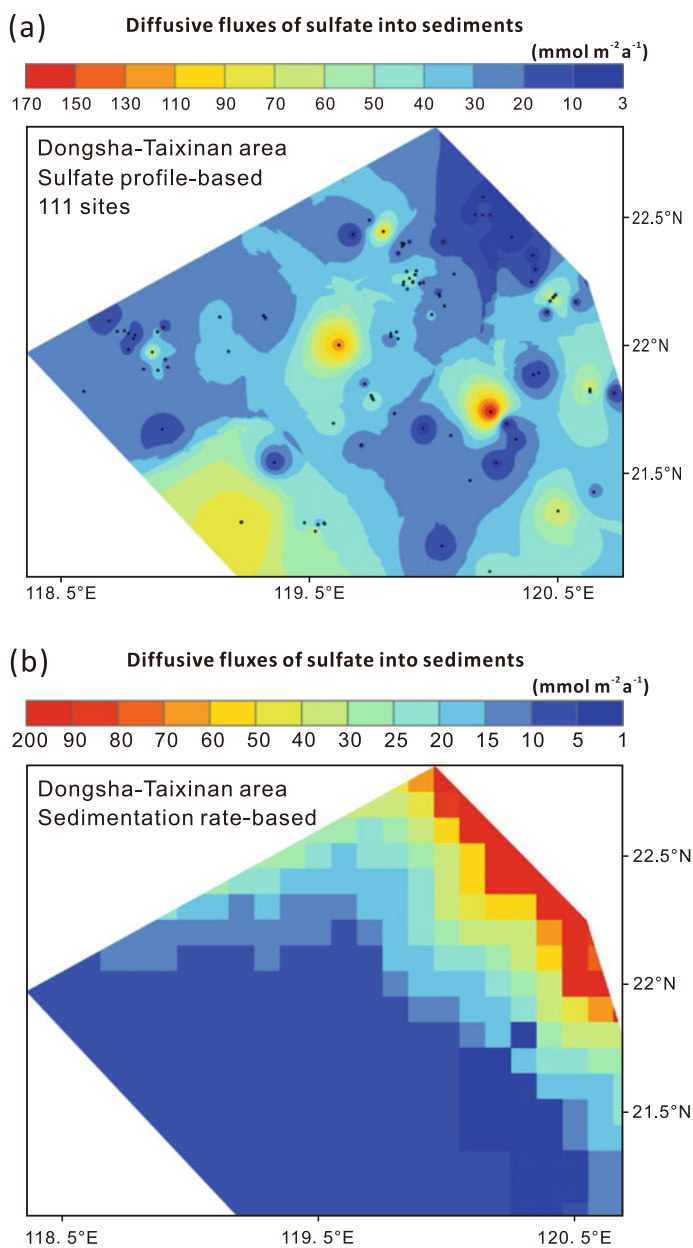


Fig. 8.9 Maps showing the distribution and magnitude of the regional sulfate flux of the Dongsha-Taixinan area based on measured sulfate profiles at 111 sites (a) and sedimentation rates (b), respectively (Modified from Hu et al. 2023)

and (2) sulfate consumed by AOM at the SMTZ that oxidizes methane fueled by local archaeal methanogenesis through organic matter fermentation below the SMTZ (Hu et al. 2022; Fig. 8.6a). Accordingly, the difference between the regional sulfate fluxes derived from sulfate profiles and those derived from sedimentation rates represents the amount of deep-sourced methane that mainly originated from deep gas hydrate reservoirs and/or deep strata kilometers below the seafloor (Hu et al. 2022).

Regional maps of sulfate flux distribution based on sedimentation rates in the northern SCS were extracted from an established, global map of sulfate flux distribution or generated from locally measured sedimentation rates (Egger et al. 2018; Hu et al. 2022, 2023; Figs. 8.8b, 8.9b and 8.10b). Accordingly, regional sulfate fluxes derived from sedimentation rate in the Dongsha–Taixinan, Shenhu, and Qiongdongnan areas are 0.54×10^{-3} , 0.30×10^{-3} , and 0.39×10^{-3} Tmol a^{-1} , respectively (Hu et al. 2022, 2023; Figs. 8.8–8.11). Based on the discrepancy between regional sulfate flux estimated from sulfate profiles and that estimated from sedimentation rates, estimated fluxes of deep-sourced methane in the Dongsha–Taixinan, Shenhu, and Qiongdongnan areas reach 0.53×10^{-3} , 0.24×10^{-3} , and 2.26×10^{-3} Tmol a^{-1} (Hu et al. 2022, 2023; Fig. 8.11). Summing up these areas, 4.26×10^{-3} Tmol of sulfate and 3.03×10^{-3} Tmol of deep-sourced methane are annually consumed in the subseafloor sediments of the northern SCS for an area of 1.23×10^5 km² (Hu et al. 2023; Fig. 8.11).

Ratios between regional flux of deep-sourced methane and regional flux of sulfate based on sulfate profiles represent the contribution of sulfate consumption by ascending deep-sourced methane to total sulfate consumption (Fig. 8.11). These ratios can be used to evaluate the overall impact of ascending deep-sourced methane on the sulfate budget in subseafloor sediments on a regional scale. The ratios reach 50%, 44%, and 85% in the Dongsha–Taixinan, Shenhu, and Qiongdongnan areas, respectively, with the overall ratio for the three study areas accounting for 71% (Hu et al. 2023; Fig. 8.11). These ratios indicate that the contribution of ascending deep-sourced methane to sulfate consumption is similar to or even higher than the contribution of organoclastic sulfate reduction on regional scales in the subseafloor sediments of the northern SCS (Hu et al. 2023). By extrapolating the results of the northern SCS to global slope and rise sediments, 2.18 to 2.65 Tmol of deep-sourced methane is oxidized with sulfate by AOM annually in marine sediments (Hu et al. 2023). Despite a rough extrapolation, it becomes obvious that deep-sourced methane plays a crucial role in subseafloor carbon and sulfur cycling, supporting chemosynthesis-based ecosystems along the continental slope and rise sediments worldwide (Hu et al. 2023).

8.6 Summary and Perspectives

Pore water profiles from more than 250 sites within gas hydrate and cold seep areas of the SCS in the past two decades were investigated to indicate fluid sources, to identify the AOM and fluid flow patterns, and to quantify AOM rates and regional methane

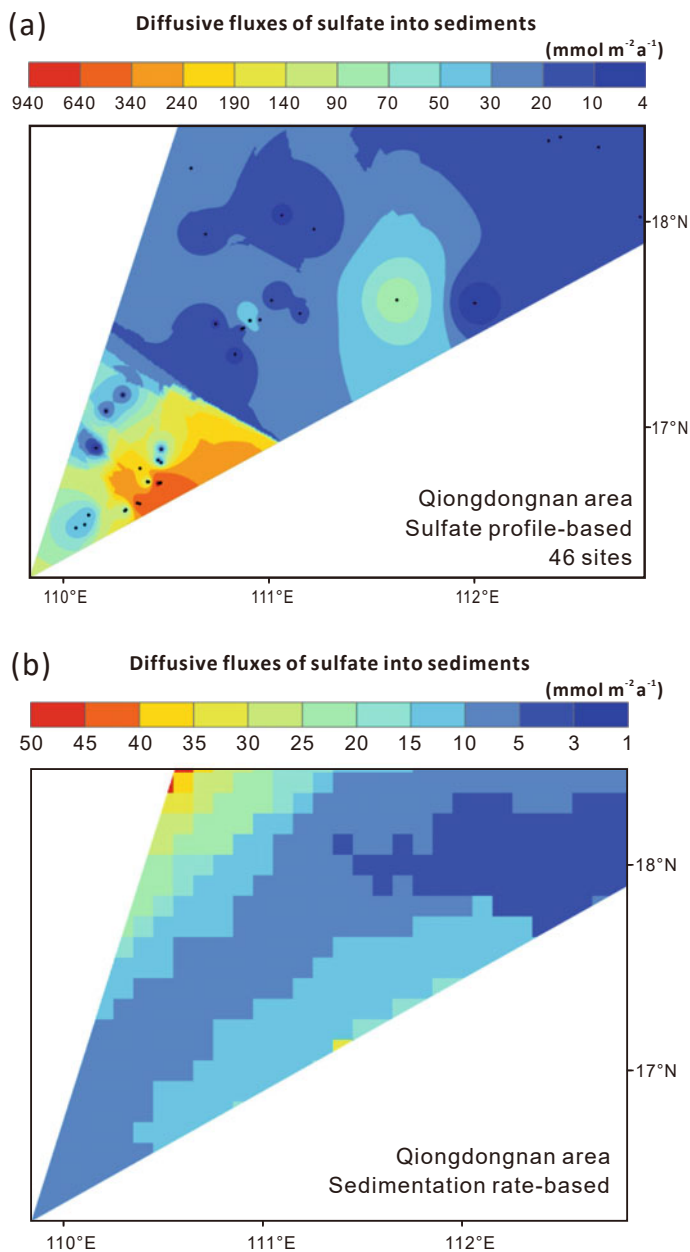


Fig. 8.10 Maps showing the distribution and magnitude of the regional sulfate flux of the Qiongdongnan area based on measured sulfate profiles at 46 sites (a) and sedimentation rates (b), respectively (Modified from Hu et al. 2023)

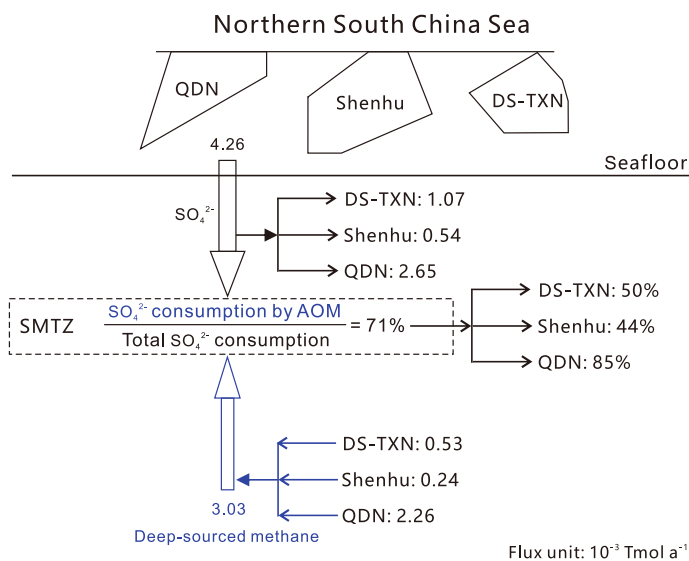


Fig. 8.11 A summary of regional sulfate (SO_4^{2-}) and methane budgets and the role of deep-sourced methane in the subsurface sediments of the northern South China Sea (Modified from Hu et al. 2023). SMTZ: sulfate-methane transition zone. AOM: anaerobic oxidation of methane. DS-TXN: Dongsha-Taixinan. QDN: Qiongdongnan

cycling. Regional sulfate budgets suggest that deep-sourced methane plays a crucial role in governing subsurface carbon and sulfur cycling along continental margins. A unique feature of the SCS is indicated by the development of a transition from an active to a passive continental margin. Does this tectonic feature in the Dongsha-Taixinan area influence the distribution and fluxes of sulfate and methane across the tectonic transition? Addressing this issue would provide a great opportunity to understand upward diffusion and/or seepages of methane on regional scales in response to tectonic activity. Although the amount of deep-sourced methane in the northern SCS has been quantified, the impact of such an amount of deep-sourced methane on subsurface carbon cycling has not been quantitatively assessed. More work is required to quantitatively evaluate the amounts of authigenic carbonate that is produced and the dissolved inorganic carbon that enters the ocean after the deep-sourced methane is oxidized with sulfate by AOM.

Acknowledgements The author gratefully acknowledges the scientists, crews, and organizers of the research vessel *Haiyang-04* and *Haiyang-06* for sampling during several research cruises in the past decade. Min Luo is acknowledged for constructive comments on this chapter. The work is partially supported by the Shanghai Pujiang Program (Grant No 21PJ1404700).

References

- Antler G, Turchyn AV, Herut B et al (2015) A unique isotopic fingerprint of sulfate-driven anaerobic oxidation of methane. *Geology* 43(7):619–622
- Boetius A, Ravensschlag K, Schubert CJ et al (2000) A marine microbial consortium apparently mediating anaerobic oxidation of methane. *Nature* 407(6804):623–626
- Burdige DJ, Komada T (2013) Using ammonium pore water profiles to assess stoichiometry of deep remineralization processes in methanogenic continental margin sediments. *Geochem Geophys Geosyst* 14(5):1626–1643
- Cao C, Lei H (2012) Geochemical characteristics of pore water in shallow sediments from north continental slope of South China Sea and their significance for natural gas hydrate occurrence. *Procedia Environmental Sciences* 12, Part B:1017–1023
- Chatterjee S, Dickens GR, Bhatnagar G et al (2011) Pore water sulfate, alkalinity, and carbon isotope profiles in shallow sediment above marine gas hydrate systems: A numerical modeling perspective. *J Geophys Res-Solid Earth* 116:B09103
- Chen N, Yang T, Hong W et al (2017) Production, consumption, and migration of methane in accretionary prism of southwestern Taiwan. *Geochem Geophys Geosyst* 18(8):2970–2989
- Chuang PC, Dale AW, Wallmann K et al (2013) Relating sulfate and methane dynamics to geology: Accretionary prism offshore SW Taiwan. *Geochem Geophys Geosyst* 14(7):2523–2545
- Chuang P, Yang T, Hong W et al (2010) Estimation of methane flux offshore SW Taiwan and the influence of tectonics on gas hydrate accumulation. *Geofluids* 10(4):497–510
- Chuang P, Yang T, Lin S et al (2006) Extremely high methane concentration in bottom water and cored sediments from offshore southwestern Taiwan. *Terr Atmos Ocean Sci* 17(4):903–920
- Deng X, Fu S, Huang Y et al (2006) Geochemical characteristics of sediments at Site HD196 in Dongsha Islands, the North of the South China Sea, and their implication for gas hydrates. *Geoscience* 20(1):92–102 (in Chinese with English abstract)
- Egger M, Riedinger N, Mogollón JM et al (2018) Global diffusive fluxes of methane in marine sediments. *Nat Geosci* 11(6):421–425
- Feng J, Yang S, Sun X et al (2018a) Geochemical tracers for methane microleakage activity in the Qiongdongnan Basin. *Journal of Southwest Petroleum University (science & Technology Edition)* 40:63–75 (in Chinese with English abstract)
- Feng J, Yang S, Liang J et al (2018b) Methane seepage inferred from the porewater geochemistry of shallow sediments in the Beikang Basin of the southern South China Sea. *J Asian Earth Sci* 168:77–86
- Feng J, Yang S, Wang H et al (2019) Methane source and turnover in the shallow sediments to the west of Haima cold seeps on the northwestern slope of the South China Sea. *Geofluids* 2019:1010824
- Feng J, Li N, Luo M et al (2020) A quantitative assessment of methane-derived carbon cycling at the cold seeps in the northwestern South China Sea. *Minerals* 10(3):256
- Feng J, Li N, Liang J (2021) Using multi-proxy approach to constrain temporal variations of methane flux in methane-rich sediments of the southern South China Sea. *Mar Pet Geol* 132:105152
- Fossing H, Ferdelman TG, Berg P (2000) Sulfate reduction and methane oxidation in continental margin sediments influenced by irrigation (South-East Atlantic off Namibia). *Geochim Cosmochim Acta* 64(5):897–910
- Gong S, Feng D, Peng Y et al (2021) Deciphering the sulfur and oxygen isotope patterns of sulfate-driven anaerobic oxidation of methane. *Chem Geol* 581:120394
- Haeckel M, Boudreau BP, Wallmann K et al (2007) Bubble-induced porewater mixing: A 3-D model for deep porewater irrigation. *Geochim Cosmochim Acta* 71(21):5135–5154
- Hensen C, Zabel M, Pfeifer K et al (2003) Control of sulfate pore-water profiles by sedimentary events and the significance of anaerobic oxidation of methane for the burial of sulfur in marine sediments. *Geochim Cosmochim Acta* 67(14):2631–2647

- Hu CY, Yang TF, Burr GS et al (2017) Biogeochemical cycles at the sulfate-methane transition zone (SMTZ) and geochemical characteristics of the pore fluids offshore southwestern Taiwan. *J Asian Earth Sci* 149:172–183
- Hu T, Luo M, Xu Y et al (2021) Production of labile protein-like dissolved organic carbon associated with anaerobic methane oxidization in the Haima cold seeps, South China Sea. *Front Mar Sci* 8:797084
- Hu Y, Luo M, Chen L et al (2018) Methane source linked to gas hydrate system at hydrate drilling areas of the South China Sea: Porewater geochemistry and numerical model constraints. *J Asian Earth Sci* 168:87–95
- Hu Y, Feng D, Liang Q et al (2015) Impact of anaerobic oxidation of methane on the geochemical cycle of redox-sensitive elements at cold-seep sites of the northern South China Sea. *Deep-Sea Res Part II-Top Stud Oceanogr* 122:84–94
- Hu Y, Luo M, Liang Q et al (2019) Pore fluid compositions and inferred fluid flow patterns at the Haima cold seeps of the South China Sea. *Mar Pet Geol* 103:29–40
- Hu Y, Feng D, Peckmann J et al (2020) The impact of diffusive transport of methane on pore-water and sediment geochemistry constrained by authigenic enrichments of carbon, sulfur, and trace elements: A case study from the Shenhu area of the South China Sea. *Chem Geol* 553:119805
- Hu Y, Feng D, Peckmann J et al (2023) The crucial role of deep-sourced methane in maintaining the seafloor sulfate budget. *Geosci Front* 14:101530
- Hu Y, Zhang X, Feng D et al (2022) Enhanced sulfate consumption fueled by deep-sourced methane in a hydrate-bearing area. *Sci Bull* 67(2):122–124
- Huang Y, Suess E, Wu N et al (2008) Methane and gas hydrate geology of the Northern South China Sea: Sino-German Cooperative SO-177 Cruise Report (in Chinese). Geological Publishing House, Beijing
- Hong WL, Torres ME, Kim JH et al (2013) Carbon cycling within the sulfate-methane-transition-zone in marine sediments from the Ulleung Basin. *Biogeochemistry* 115(1–3):129–148
- Huang W, Meng M, Zhang W et al (2022) Geological, geophysical, and geochemical characteristics of deep-routed fluid seepage and its indication of gas hydrate occurrence in the Beikang Basin, Southern South China Sea. *Mar Pet Geol* 139:105610
- Jiang S, Yang T, Xue Z et al (2005) Chlorine and sulfate concentrations in pore-waters from marine sediments in the north margin of the South China Sea and their implications for gas hydrate exploration. *Geoscience* 19(1):45–54 (in Chinese with English abstract)
- Jin M, Feng D, Huang K et al (2022) Magnesium isotopes in pore water of active methane seeps of the South China Sea. *Front Mar Sci* 9:858860
- Kasten S, Zabel M, Heuer V et al (2003) Processes and signals of nonsteady-state diagenesis in deep-sea sediments and their pore waters. In: Wefer G, Mulitza S, Ratmeyer V (eds) *The South Atlantic in the Late Quaternary: Reconstruction of Material Budget and Current Systems*. Springer, Berlin, pp 431–459
- Kim JH, Park MH, Chun JH et al (2011) Molecular and isotopic signatures in sediments and gas hydrate of the central/southwestern Ulleung Basin: high alkalinity escape fuelled by biogenically sourced methane. *Geo-Mar Lett* 31(1):37–49
- Komada T, Burdige DJ, Magen C et al (2016) Recycling of organic matter in the sediments of Santa Monica Basin California Borderland. *Aquat Geochem* 22(5–6):593–618
- Lin S, Hsieh W, Lim YC et al (2006) Methane migration and its influence on sulfate reduction in the Good Weather Ridge region, South China Sea continental margin sediments. *Terr Atmos Ocean Sci* 17(17):883–902
- Liu W, Wu Z, Xu S et al (2020) Pore-water dissolved inorganic carbon sources and cycling in the shallow sediments of the Haima cold seeps, South China Sea. *J Asian Earth Sci* 201:104495
- Luo M, Chen L, Wang S et al (2013) Pockmark activity inferred from pore water geochemistry in shallow sediments of the pockmark field in southwestern Xisha Uplift, northwestern South China Sea. *Mar Pet Geol* 48:247–259

- Luo M, Chen L, Tong H et al (2014) Gas hydrate occurrence inferred from dissolved Cl⁻ concentrations and δ¹⁸O values of pore water and dissolved sulfate in the shallow sediments of the pockmark field in southwestern Xisha uplift, northern South China Sea. *Energies* 7(6):3886–3899
- Liang Q, Hu Y, Feng D et al (2017) Authigenic carbonates from newly discovered active cold seeps on the northwestern slope of the South China Sea: Constraints on fluid sources, formation environments, and seepage dynamics. *Deep-Sea Res Part I-Oceanogr Res Pap* 124:31–41
- Reeburgh WS (2007) Oceanic methane biogeochemistry. *Chem Rev* 107(2):486–513
- Sha Z, Liang J, Zhang G et al (2015) A seepage gas hydrate system in northern South China Sea: Seismic and well log interpretations. *Mar Geol* 366:69–78
- Schulz HD (2006) Schulz HD, Zabel M (Eds) Quantification of early diagenesis: dissolved constituents in pore water and signals in the solid phase. *Marine Geochemistry*. Berlin, Germany, pp. 73–124
- Suess E (2005) RV SONNE Cruise Report SO 177, Sino-German Cooperative Project, South China Sea Continental Margin: Geological Methane Budget and Environmental Effects of Methane Emissions and Gas Hydrates. IFM-GEOMAR Reports. https://doi.org/10.3289/ifm-geomar_rep_4_2005
- Wang X, Li N, Feng D et al (2018) Using chemical compositions of sediments to constrain methane seepage dynamics: A case study from Haima cold seeps of the South China Sea. *J Asian Earth Sci* 168:137–144
- Wei J, Liang J, Lu J et al (2019) Characteristics and dynamics of gas hydrate systems in the northwestern South China Sea – Results of the fifth gas hydrate drilling expedition. *Mar Pet Geol* 110:287–298
- Wu D, Wu N, Zhang M et al (2013a) Relationship of sulfate-methane interface (SMI), methane flux and the underlying gas hydrate in Dongsha area, Northern South China Sea. *Earth Science-J China Univ Geosci* 38(6):1309–1320 (in Chinese with English abstract)
- Wu LS, Yang SX, Liang JQ et al (2013b) Variations of pore water sulfate gradients in sediments as indicator for underlying gas hydrate in Shenhu Area, the South China Sea. *Sci China-Earth Sci* 56(4):530–540
- Wu LS, Yang SX, Liang JQ et al (2010) Geochemical characteristics of sediments at site HQ-48PC in Qiongdongnan Area, the north of the South China Sea, and their implication for gas hydrates. *Geoscience* 24(3):534–544 (in Chinese with English abstract)
- Wu N, Ye Y, Wu D et al (2007) Geochemical characteristic of sediments from Southeast Hainan Basin, South China Sea and micro-methane-seep activity. *Geology Res South China Sea* 00:40–47 (in Chinese with English abstract)
- Wu N, Zhang H, Yang S et al (2011) Gas Hydrate System of Shenhu Area, Northern South China Sea: Geochemical Results. *J Geol Res* 2011:370298
- Yang T, Jiang S, Ge L et al (2006) Geochemical characteristics of sediment pore water from Site XS-01 in the Xisha trough of South China Sea and their significance for gas hydrate occurrence. *Quaternary Sciences* 3:442–448 (in Chinese with English abstract)
- Yang T, Jiang SY, Yang JH et al (2008a) Dissolved inorganic carbon (DIC) and its carbon isotopic composition in sediment pore waters from the Shenhu area, northern South China Sea. *J Oceanogr* 64(2):303–310
- Yang SX, Zhang HQ, Wu NY et al (2008b) High concentration hydrate in disseminated forms obtained in Shenhu area, North Slope of South China Sea. Vancouver BC. (Canada) In: 6th International Conference on Gas Hydrates (ICGH 2008), 6–10 July 2008, pp 1–6
- Yang T, Jiang SY, Ge L et al (2013) Geochemistry of pore waters from HQ-1PC of the Qiongdongnan Basin, northern South China Sea, and its implications for gas hydrate exploration. *Sci China-Earth Sci* 56(4):521–529
- Yang S, Zhang M, Liang J et al (2015) Preliminary results of China's third Gas hydrate drilling expedition: a critical step from discovery to development in the South China Sea. *Fire Ice* 15:1–5
- Ye H, Yang T, Zhu G et al (2016) Pore water geochemistry in shallow sediments from the northeastern continental slope of the South China Sea. *Mar Pet Geol* 75:68–82

- Ye J, Wei J, Liang J et al (2019) Complex gas hydrate system in a gas chimney, South China Sea. *Mar Pet Geol* 104:29–39
- Zabel M, Schulz HD (2001) Importance of submarine landslides for non-steady state conditions in pore water systems – lower Zaire (Congo) deep-sea fan. *Mar Geol* 176(1–4):87–99
- Zha R, Yang T, Shi X et al (2022) Quantitative assessment of dissolved inorganic carbon cycling in marine sediments from gas hydrate-bearing areas in the South China Sea. *Mar Pet Geol* 145:105881
- Zhang J, Lei H, Ou W et al (2014) Research of the sulfate-methane transition zone (SMTZ) in sediments of 973–4 column in continental slope of Northern South China Sea. *Nat Gas Geosci* 25(11):1811–1820 (in Chinese with English abstract)
- Zhang G, Liang J, Lu J et al (2015) Geological features, controlling factors and potential prospects of the gas hydrate occurrence in the east part of the Pearl River Mouth Basin, South China Sea. *Mar Pet Geol* 67:356–367
- Zhang W, Liang J, Liang Q et al (2021) Gas hydrate accumulation and occurrence associated with cold seep systems in the northern South China Sea: An overview. *Geofluids* 2021:5571150
- Zhang Y, Luo M, Hu Y et al (2019) An areal assessment of subseafloor carbon cycling in cold seeps and hydrate-bearing areas in the northern South China Sea. *Geofluids* 2019:1–14
- Zhuang GC, Xu L, Liang Q et al (2019) Biogeochemistry, microbial activity, and diversity in surface and subsurface deep-sea sediments of South China Sea. *Limnol Oceanogr* 64(5):2252–2270

Open Access This chapter is licensed under the terms of the Creative Commons Attribution 4.0 International License (<http://creativecommons.org/licenses/by/4.0/>), which permits use, sharing, adaptation, distribution and reproduction in any medium or format, as long as you give appropriate credit to the original author(s) and the source, provide a link to the Creative Commons license and indicate if changes were made.

The images or other third party material in this chapter are included in the chapter's Creative Commons license, unless indicated otherwise in a credit line to the material. If material is not included in the chapter's Creative Commons license and your intended use is not permitted by statutory regulation or exceeds the permitted use, you will need to obtain permission directly from the copyright holder.

